

RSC Advances



This is an *Accepted Manuscript*, which has been through the Royal Society of Chemistry peer review process and has been accepted for publication.

Accepted Manuscripts are published online shortly after acceptance, before technical editing, formatting and proof reading. Using this free service, authors can make their results available to the community, in citable form, before we publish the edited article. This *Accepted Manuscript* will be replaced by the edited, formatted and paginated article as soon as this is available.

You can find more information about *Accepted Manuscripts* in the [Information for Authors](#).

Please note that technical editing may introduce minor changes to the text and/or graphics, which may alter content. The journal's standard [Terms & Conditions](#) and the [Ethical guidelines](#) still apply. In no event shall the Royal Society of Chemistry be held responsible for any errors or omissions in this *Accepted Manuscript* or any consequences arising from the use of any information it contains.

1 **Bioreceptor multi-walled carbon nanotubes@Fe₃O₄@SiO₂-surface**
2 **molecular imprinted polymer in ultrasensitive chemiluminescence**
3 **biosensing bovine hemoglobin**

4 Huimin Duan, Xiaojiao Wang, Yanhui Wang, Jianbo Li, Chuannan Luo*

5 Key Laboratory of Chemical Sensing & Analysis in Universities of Shandong (University of
6 Jinan), School of Chemistry and Chemical Engineering, University of Jinan, Jinan 250022, China

7 * Corresponding author. Tel.: +86 0531 89736065. E-mail address: chm_luocn@ujn.edu.cn.

8 **Abstract**

9 An ultrasensitive chemiluminescence (CL) biosensor with high selectivity based
10 on bioreceptor surface molecular imprinted polymer (SMIP) which using core-shell
11 Fe₃O₄@SiO₂-multi-walled carbon nanotubes nanostructures (Fe₃O₄@SiO₂/MWCNTs)
12 as backbone materials for bovine hemoglobin (Bhb) was proposed. The
13 Fe₃O₄@SiO₂/MWCNTs was synthesized with a new method, and then was
14 characterized by SEM, FTIR and XRD techniques. Adsorption ability of the
15 Fe₃O₄@SiO₂/MWCNTs-SMIP was evaluated to be 91 mg/g and
16 Fe₃O₄@SiO₂/MWCNTs-SMIP followed Langmuir isotherm equation and it
17 demonstrated the excellent recognition and adsorption ability for the imprinted sites
18 which located on the surface or near the surface of the Fe₃O₄@SiO₂/MWCNTs. Under
19 the optimum conditions of CL, the detection range of Bhb was from 5.0×10^{-10} to 7.0
20 $\times 10^{-7}$ mg/mL with the detection limit of 1.5×10^{-10} mg/mL (3δ). The proposed
21 biosensor was successfully applied in determination of Bhb in real samples with high
22 selectivity and sensitivity, and the recoveries were excellent and varied from 92% to
23 106%. Finally, the possible CL mechanism of the Bhb amplifying the CL signal of
24 luminol-NaOH-H₂O₂ system was discussed.

25 **Keyword:** chemiluminescence biosensor; surface molecular imprinted polymer; bioreceptor;

26 multi-walled carbon nanotubes; Fe₃O₄@SiO₂; bovine hemoglobin

27 **1. Introduction**

28 Chemiluminescence (CL), usually coupled with chemical reaction process, was a
29 radiation phenomenon which liberated energy by light emission. For the past few
30 years, bioimaging, pharmaceutical and environmental analysis et al. [1] has confirmed
31 the importance of CL technique due to its high sensitivity, no background interference
32 and simple instrument. However, the extensive application of CL was still restricted
33 owing to its low selectivity which could be improved by molecular imprinting [2].

34 In the early 1970s, Wulff et al. [3] proposed molecular imprinting technique
35 which made the selectivity to target molecules improved greatly. A higher accuracy
36 and lower detection limit were achieved for Wulff's contribution in the substance
37 analyses for the preparation of polymer with specific cavities decorated with
38 functional groups [4]. Then, the whole century witnessed the booming of molecular
39 imprinting technique. Although selectivity to small molecules could be improved, the
40 preparation of molecularly imprinted polymer (MIP) for biomacromolecules, such as
41 proteins, remained a challenge. In 1987, Keyes [5] and Dabulis [6] et al. have studied
42 bioimprinting respectively. Surface molecular imprinting technique was synthesizing
43 a polymer attaching the biomolecule to the surface or in the proximity of the surface
44 of the polymer, which made the mass transfer improved and the removal of the
45 template biomolecule promoted [7]. Atom transfer radical polymerization, discovered
46 by Kato et al. [8], was introduced in the preparation of surface molecular imprinting
47 polymer (SMIP) bioreceptor [9].

48 Fe₃O₄ nanoparticles (NPs) were superior stabilizer and separation reagent used in
49 many fields [10] because of their good biocompatibility, low toxicity, stable physical
50 properties and easy preparation. In 2011, Gao et al. successfully prepared magnetic

51 SMIP on the surface of Fe_3O_4 NPs which served as the support materials to prepare
52 biomolecule imprinted polymer by imprinting bovine serum albumin, ribonuclease A
53 and lysozyme [11]. Si NPs, as one of the most promising one-dimensional materials,
54 were applied in sensors, batteries, catalysts and so on for their particular properties. In
55 2010, He et al. synthesized SMIP over vinyl modified silica NPs via surface graft
56 copolymerization using low monomer concentration, which was in aqueous media
57 with lysozyme as template protein [12]. When deposited on the surface of Fe_3O_4 NPs,
58 SiO_2 NPs possessed abundant carboxylic groups that could immobilize protein
59 template. $\text{Fe}_3\text{O}_4@\text{SiO}_2$ SMIP exhibited high adsorption capacity to the biomolecular
60 and adsorption equilibrium could be easily reached, and SMIP could be separated
61 easily using an external magnetic field [13]. Carbon nanotubes, which were one
62 dimensional quantum materials, had extraordinary biocompatible, mechanical and
63 electrical properties. And then, Zhang et al. prepared MIP on the surface of
64 MWCNTs- Fe_3O_4 composite [14].

65 Hemoglobin (Hb) was the main undertaker of organic life for a variety of
66 physiological activities. It played critical roles in the transportation of oxygen and
67 carbon dioxide and maintenance of the pH balance in the blood stream of the vascular
68 system [15]. The structure of Hb on its transport oxygen function made respiratory
69 function efficient. Dysregulation of the structure of Hb in its four molecular subunits
70 could result in various kinds of hereditary diseases, such as sickle cell anemia,
71 thalassemia and so on [16]. Thus, the analysis of Hb was of important significance.
72 While bovine hemoglobin (BHb) shared 90% similarities with human hemoglobin
73 [17], we could make BHb as the target protein in the analysis of Hb. During the past
74 decades, many methods have been reported on the determination of BHb, for example,
75 electrochemical methods [18, 19], fluorescence method [20] and piezoelectric crystal

76 immunosensor [21].

77 This work proposed an ultrasensitive chemiluminescence (CL) biosensor to BHb.
78 The nanocomplex of Fe₃O₄ NPs, SiO₂ NPs and MWCNTs was served as backbone
79 materials simultaneously to prepare bioreceptor SMIP for the CL biosensor for highly
80 sensitive detection of BHb. In brief, Fe₃O₄@SiO₂ was not only served as backbone
81 material to prepare BHb SMIP, but also as separation material to separate SMIP
82 complex and MWCNTs was used as supporting material to bear Fe₃O₄@SiO₂ and
83 prepare SMIP for their large specific surface area. Adsorption ability of the
84 Fe₃O₄@SiO₂/MWCNTs-SMIP to BHb was researched, and
85 Fe₃O₄@SiO₂/MWCNTs-SMIP followed Langmuir isotherm equation and it exhibited
86 excellent recognition and adsorption ability to BHb owing to the imprinted sites
87 located on the surface or near the surface of the Fe₃O₄@SiO₂/MWCNTs. Finally,
88 based on Fe₃O₄@SiO₂/MWCNTs-SMIP bioreceptor, the proposed CL biosensor was
89 successfully applied in detection of BHb in samples with high sensitivity and
90 selectivity under the optimum conditions of CL.

91 **2 Experiment**

92 **2.1 Chemicals and materials**

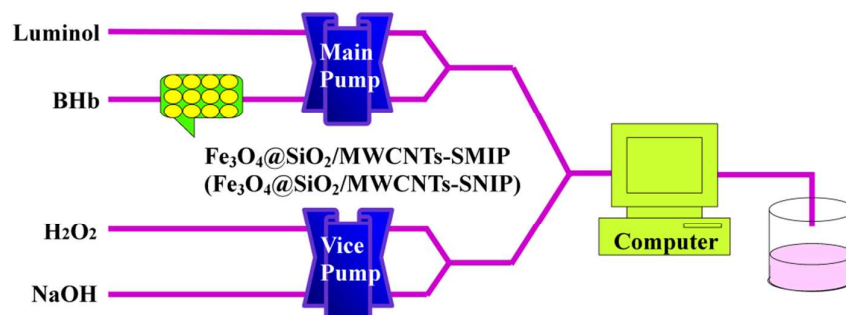
93 Anhydrous tetrahydrofuran (99%), N-N methylene double acrylamide (MBA,
94 A.R), N,N,N',N'-tetramethyl ethylenediamine (TEMED, A.R), Diethyl amino ethyl
95 methacrylate (DMAEMA, 99%) and 3-aminopropyltrimethoxysilane (AMPS, 97%)
96 were purchased from Aladdin Industrial Co. (China); Thionyl chloride (A.R),
97 Tetraethyl silicate (TEOS, A.R), Ferrous sulfate(A.R), Dimethyl formamide (DMF,
98 99%), Acrylamide (AM, 99%), Methacrylic acid (MAA), and Ammonium
99 persulphate (APS, AR) were supplied by Sinopharm Chemical Reagent Co. Ltd
100 (China); MWCNTs was obtained from Beijing Dk Nano technology Co., Ltd (China);

101 BHB were acquired from Shanghai Reagent Co. (China). The ethanol, acetic acid,
102 methanol, luminol and all the other chemicals unless specified were of analytical
103 reagent grade and used without further purification.

104 TEOS and DMF were distilled reduced vacuum pressure and DMAEMA was
105 purified with alkaline Al_2O_3 column. Redistilled water was used throughout the work.
106 Phosphate buffer (PBS, pH=7.4, 0.02 mol/L) solution was used to prepare all BHB
107 solutions which were stored in refrigerator (4°C).

108 **2.3 Apparatus**

109 The IFFM-E flow injection CL analyser (Xi'an Remex Electronic instrument
110 High-Tech Ltd., China) was equipped with an automatic injection system and a
111 detection system. PTFE tubes (0.8 mm i.d.) were used to connect all of the
112 components in the flow system. Capillary filled with a certain amount
113 $\text{Fe}_3\text{O}_4@\text{SiO}_2/\text{MWCNTs-SMIP}$ bioreceptor and non-imprinted polymer
114 ($\text{Fe}_3\text{O}_4@\text{SiO}_2/\text{MWCNTs-SNIP}$) bioreceptor was collected with pump by PTFE tubes
115 and was placed in front of the CL analyser as recognition elements as shown in Fig. 1.
116 When BHB solution ran through the capillary, BHB molecule could be absorbed by
117 $\text{Fe}_3\text{O}_4@\text{SiO}_2/\text{MWCNTs-SMIP}$ selectivity, a CL signal I_0 was obtained, while
118 $\text{Fe}_3\text{O}_4@\text{SiO}_2/\text{MWCNTs-SNIP}$ could not absorb BHB molecule, another CL signal I_1
119 was obtained. Then the difference $\Delta I = I_1 - I_0$ was the concentration of BHB in the
120 linear relationship. XRD measurement was made on a D8 focus spectrometer (Brooke
121 AXS, Germany). FT-IR spectrometer (PerkinElmer, USA) was employed to confirm
122 the products. A FEI QUANTA FEG250 field emission scanning electron microscopy
123 (SEM, USA) was employed to observe the morphology of the nanoparticles.



124

125 **Fig.1.** The mechanism of CL biosensor based on $\text{Fe}_3\text{O}_4@\text{SiO}_2/\text{MWCNTs-SMIP}$ bioreceptor

126 2.3 Preparation of $\text{Fe}_3\text{O}_4@\text{SiO}_2$

127 $\text{Fe}_3\text{O}_4@\text{SiO}_2$ was synthesized according to a modified procedure described in the
128 previous literatures [22] and our group [23].

129 $\text{FeCl}_2 \cdot 4\text{H}_2\text{O}$ (35 mg) and $\text{FeCl}_3 \cdot 6\text{H}_2\text{O}$ (50 mg) were dissolved in 80 mL of water
130 with vigorous stirring under nitrogen protection. 10 mL of $\text{NH}_4 \cdot \text{OH}$ (28 wt. %) was
131 added into the system drop by drop, and the reaction was maintained at 80 °C for 30
132 min. The black precipitation was separated with an external magnetic field, and
133 washed with water and ethanol to remove the unreacted chemicals, and then dried in
134 the vacuum at 60 °C. Subsequently, 0.3 g of as prepared Fe_3O_4 NPs were dispersed in
135 36 mL of ethanol and 4 mL of ultrapure water by ultrasonication for 15 min in 150
136 mL round bottom flask, followed by the addition of 10 mL of $\text{NH}_4 \cdot \text{OH}$ and 5 mL of
137 TEOS. The mixtures were reacted for 12 h at room temperature by constant
138 mechanism stirring. The products ($\text{Fe}_3\text{O}_4@\text{SiO}_2$) were collected by magnetic
139 separation, washed with water and ethanol, and then dried in the vacuum at 50 °C.

140 2.4 Preparation of $\text{Fe}_3\text{O}_4@\text{SiO}_2/\text{MWCNTs}$

141 0.5 g $\text{Fe}_3\text{O}_4@\text{SiO}_2$ NPs were dispersed in 50 mL of anhydrous toluene. Then, 5
142 mL of AMPS was added in the solution followed by refluxing at 80 °C for 16 h.
143 After magnetic separated, washed by water and ethanol, dried in vacuum, products
144 ($\text{Fe}_3\text{O}_4@\text{SiO}_2\text{-NH}_2$) were obtained.

145 The carboxylated MWCNTs (MWCNTs-COOH) were prepared by refluxing the
146 MWCNTs in a nitric acid (65-68 wt. %) at 75 °C for 11 h [24]. After cooling to room
147 temperature, the mixture was filtered and washed with double distilled water till the
148 pH=6.5 and finally dried at 60 °C overnight. 0.3 g MWCNTs-COOH was dispersed in
149 25 mL thionyl chloride solution by ultrasonication (200W, 40 kHz). The mixture was
150 further stirred vigorously and refluxed for 24 h at 50 °C. Then the product
151 (MWCNTs-COCl) was washed by anhydrous tetrahydrofuran followed dried at 50 °C.

152 10 mg of MWCNTs-COCl and 20 mg Fe₃O₄@SiO₂-NH₂ were scattered in 20
153 mL DMF by ultrasonication which then was refluxed at 120 °C for 24 h under the
154 protection of N₂. The obtained product (Fe₃O₄@SiO₂/MWCNTs) was then separated,
155 washed by water and ethanol and dried in vacuum.

156 **2.5 Preparation of Fe₃O₄@SiO₂/MWCNTs-SMIP and NIP bioreceptor**

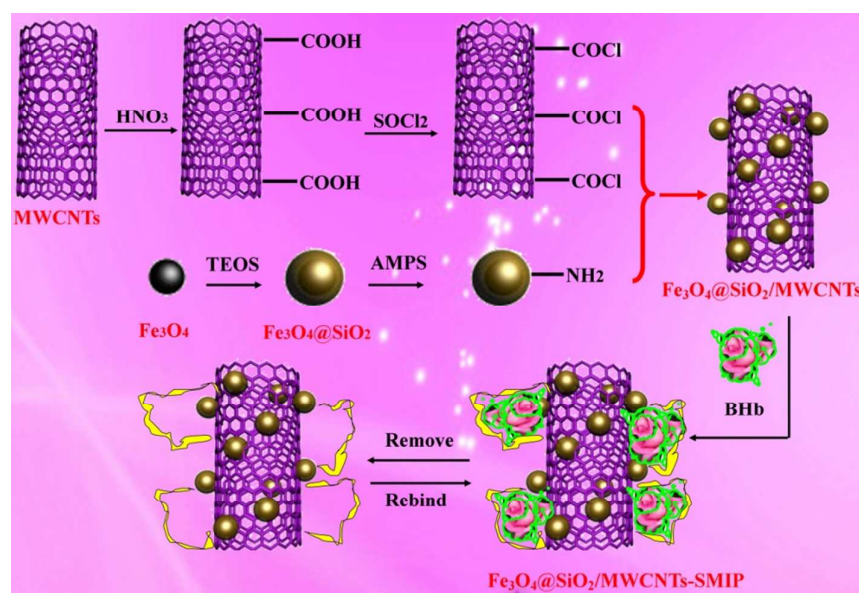
157 Fe₃O₄@SiO₂/MWCNTs-SMIP was synthesized according to a modified
158 procedure described in the previous literatures [12]. The preparing process was shown
159 in Fig. 2.

160 Solution A: AM (16 mg), MBA (32 mg), MAA (0.1 mL) and DMAEMA (0.1
161 mL) were dissolved in 25 mL of PBS solution and mixed thoroughly by
162 ultrasonication. And then, 32 mg of BHB was dissolved to this solution by sonication.

163 Solution B: 120 mg Fe₃O₄@SiO₂/MWCNTs was dispersed in 15 mL ethanol and
164 10 mL PBS solution which was then ultrasonicated to make it well-distributed.

165 After adding solution B to solution A, the mixture was degassed under vacuum
166 for 10 min and purged with nitrogen stream for another 10 min. Then, the solution
167 was incubated for 1 h to preassemble. By adding 30 mg of APS, 0.4 mL TEMED and
168 15 mg ferrous sulfate to the mixture, polymerization was initiated and continued
169 under violent stirring at 25 °C for 10 min.

170 After the reaction, the BHB-imprinted particles were collected by magnetic
 171 separation. The particles were washed with deionized water solution. And then, they
 172 were washed repeatedly with 0.5 mol/L NaCl solution to remove embedded template
 173 until no BHB in the supernatant. Subsequently, they were washed with PBS solution
 174 to remove remained NaCl solution. Finally, the $\text{Fe}_3\text{O}_4@\text{SiO}_2/\text{MWCNTs-SMIP}$
 175 bioreceptor was freeze-dried for further use. The $\text{Fe}_3\text{O}_4@\text{SiO}_2/\text{MWCNTs-SNIP}$
 176 bioreceptor were prepared and washed in the same way but without addition of BHB.



177

178 **Fig.2.** The preparing process of $\text{Fe}_3\text{O}_4@\text{SiO}_2/\text{MWCNTs-SMIP}$ bioreceptor

179 2.6 Rebinding performance of $\text{Fe}_3\text{O}_4@\text{SiO}_2/\text{MWCNTs-SMIP}$ and $\text{Fe}_3\text{O}_4@\text{SiO}_2/\text{MWCNTs-SNIP}$

181 Batch rebinding tests: 55 mg $\text{Fe}_3\text{O}_4@\text{SiO}_2/\text{MWCNTs-SMIP}$ and $\text{Fe}_3\text{O}_4@\text{SiO}_2/\text{MWCNTs-SNIP}$
 182 NPs were placed into 5 mL centrifuge tubes, respectively. The
 183 protein solutions were prepared at different initial concentration: 0.1 mg/mL, 0.2
 184 mg/mL, 0.4 mg/mL, 0.6 mg/mL, 0.8 mg/mL, 1.0 mg/mL and 1.5 mg/mL. Then, 2.0
 185 mL of each solution was added into the tube and thoroughly mixed with the particles.
 186 The dispersion liquid was incubated at 25 °C for 1 h. After magnetic separation, the

187 concentration of the supernatant in the tube was determined by CL instrument.

188 Rebinding kinetics: 55 mg $\text{Fe}_3\text{O}_4@\text{SiO}_2/\text{MWCNTs-SMIP}$ and $\text{Fe}_3\text{O}_4@\text{SiO}_2/$
189 MWCNTs-SNIP NPs were soaked in 2.0 mL 2.0 mg/mL BHB solution which then
190 was incubated at 25 °C for 1 min, 5 min, 10 min, 20 min, 30 min and 40 min. After
191 magnetic separation, the concentration of the supernatant in the tube was determined
192 by CL instrument.

193 All the tests were conducted in triplicates. The amount of protein adsorbed by the
194 particles was calculated from the following formula.

$$Q = (c_0 - c_e) \frac{V}{m}$$

195 Where Q (mg/g) was the mass of protein adsorbed by unit mass of dry particles,
196 c_0 (mg/mL) and c_e (mg/mL) were the concentrations of the initial and final solution,
197 respectively, V (mL) was the total volume of the adsorption mixture, and m (g) was
198 the mass of the $\text{Fe}_3\text{O}_4@\text{SiO}_2/\text{MWCNTs-SMIP}$ ($\text{Fe}_3\text{O}_4@\text{SiO}_2/\text{MWCNTs-SNIP}$) used.

199 2.7 Selectivity experiments of the biosensor

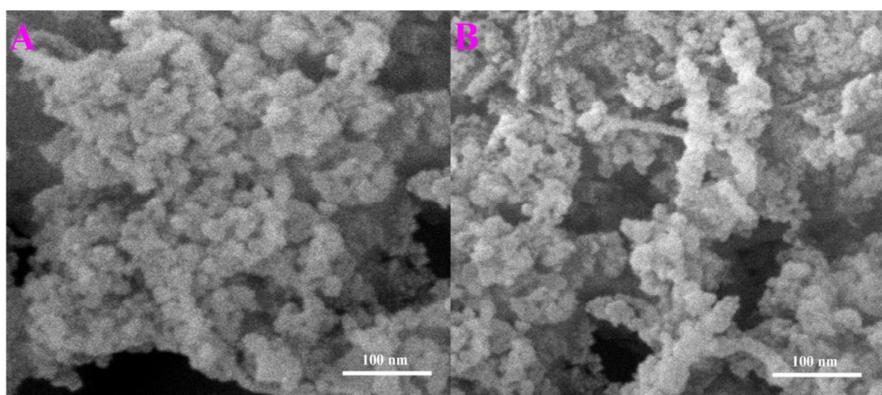
200 The selectivity experiments of the $\text{Fe}_3\text{O}_4@\text{SiO}_2/\text{MWCNTs-SMIP-CL}$ biosensor
201 was carried out with other two kinds of proteins: bovine serum albumin (BSA) and
202 lysozyme (Lys). A certain concentration of common substances and proteins were
203 added into BHB standard solution (5.0×10^{-8} mg/mL) to research the effects on the
204 CL intensity.

205 3 Results and discussion

206 3.1 Characterization of $\text{Fe}_3\text{O}_4@\text{SiO}_2$ and $\text{Fe}_3\text{O}_4@\text{SiO}_2/\text{MWCNTs}$

207 The surface morphology of the $\text{Fe}_3\text{O}_4@\text{SiO}_2$ and $\text{Fe}_3\text{O}_4@\text{SiO}_2/\text{MWCNTs}$ was
208 characterized by SEM and was shown in Fig. 3, respectively. As it shown in Fig. 3
209 (A), the image showed that the prepared $\text{Fe}_3\text{O}_4@\text{SiO}_2$ NPs were well shaped beads

210 and well dispersed. Fig. 3 (B) showed that when reacted with MWCNTs,
211 $\text{Fe}_3\text{O}_4@\text{SiO}_2$ were anchored on the surface of MWCNTs which made surface
212 molecular imprinting more favorable by improving mass transfer. Hence, we
213 considered that the $\text{Fe}_3\text{O}_4@\text{SiO}_2$ and $\text{Fe}_3\text{O}_4@\text{SiO}_2/\text{MWCNTs}$ were synthesized
214 successfully.

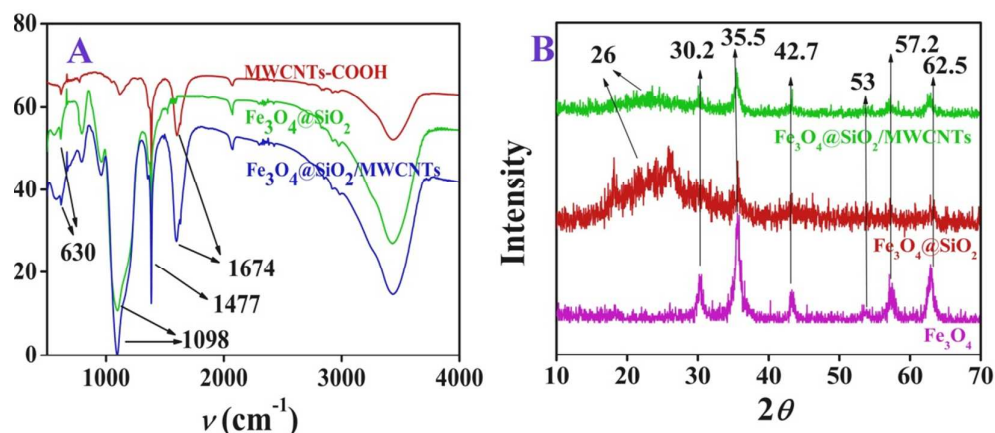


215
216 **Fig.3.** The SEM images of $\text{Fe}_3\text{O}_4@\text{SiO}_2$ (A) and $\text{Fe}_3\text{O}_4@\text{SiO}_2/\text{MWCNTs}$ (B)

217 The FTIR spectra of MWCNTs-COOH, $\text{Fe}_3\text{O}_4@\text{SiO}_2$ and $\text{Fe}_3\text{O}_4@\text{SiO}_2/$
218 MWCNTs were recorded within the range of $4000 - 500 \text{ cm}^{-1}$ and were showed in Fig.
219 4 (A). The peak at 630 cm^{-1} was the characteristic peak of Fe_3O_4 . It could be seen that
220 the stretching vibration of Si-O bond contributed to the strong absorption at 1098 cm^{-1} .
221 In the spectra of $\text{Fe}_3\text{O}_4@\text{SiO}_2/\text{MWCNTs}$, peaks at 1477 and 1674 cm^{-1} were due to
222 the stretching vibration of benzene ring and C=O respectively, which provided
223 abundant evidence of the satisfactory preparation of $\text{Fe}_3\text{O}_4@\text{SiO}_2/\text{MWCNTs}$.

224 In the XRD patterns of Fe_3O_4 , $\text{Fe}_3\text{O}_4@\text{SiO}_2$ and $\text{Fe}_3\text{O}_4@\text{SiO}_2/\text{MWCNTs}$ shown
225 in Fig.4 (B), the diffraction peaks at $2\theta = 30.2^\circ, 35.5^\circ, 42.7^\circ, 53^\circ, 57.2^\circ$ and 62.5°
226 were the six characteristic peaks of Fe_3O_4 . In the pattern of $\text{Fe}_3\text{O}_4@\text{SiO}_2/\text{MWCNTs}$,
227 the broad and obviously strong diffraction peak around $2\theta = 26^\circ$ was corresponded to
228 the MWCNTs [25] and amorphous form of SiO_2 [26], overlapping $\text{Fe}_3\text{O}_4@\text{SiO}_2$ and
229 MWCNTs, which created a wealth proof that $\text{Fe}_3\text{O}_4@\text{SiO}_2/\text{MWCNTs}$ was prepared

230 nicely.



231

232 **Fig.4.** The FTIR spectra (A) of MWCNTs-COOH, Fe₃O₄@SiO₂ and Fe₃O₄@SiO₂/MWCNTs. The

233

XRD pattern (B) of Fe₃O₄, Fe₃O₄@SiO₂ and Fe₃O₄@SiO₂/MWCNTs

234 3.2 Rebinding capacity and kinetics

235

The adsorption performance of Fe₃O₄@SiO₂/MWCNTs-SMIP and Fe₃O₄@SiO₂/

236 MWCNTs-SNIP to BHB were performed and was shown in Fig. 5. Rebinding

237

capacities to BHB at different initial concentrations, i.e. adsorption isotherms, were

238

showed in Fig. 5 (A). The adsorption capacity to BHB increased with the increasing of

239

the BHB concentration before reaching maximum 91 mg/g which was higher than that

240

of the SNIP prepared at the same conditions. Compared to the maximum adsorption

241

amount with Fe₃O₄@SiO₂/MIP 77.6 mg/g [27], silica-Fe₃O₄ NPs MIP 4.30 mg/g [28]

242

and Si-NPs/CdTe/MIP 19.7 mg/g [20], it certified that Fe₃O₄@SiO₂/MWCNTs-SMIP

243

was more advantaged to recognize BHB clearly. Theory adsorption capacity of

244

Fe₃O₄@SiO₂/MWCNTs-SMIP was described by Langmuir isotherm shown by the

245

inset of Fig. 5 (A). The adsorption to BHB was monolayer absorption on the surface

246

of Fe₃O₄@SiO₂/MWCNTs-SMIP. The theory maximum adsorption capacity to BHB

247

obtained by Langmuir isotherm was 98 mg/g which was approximate to the

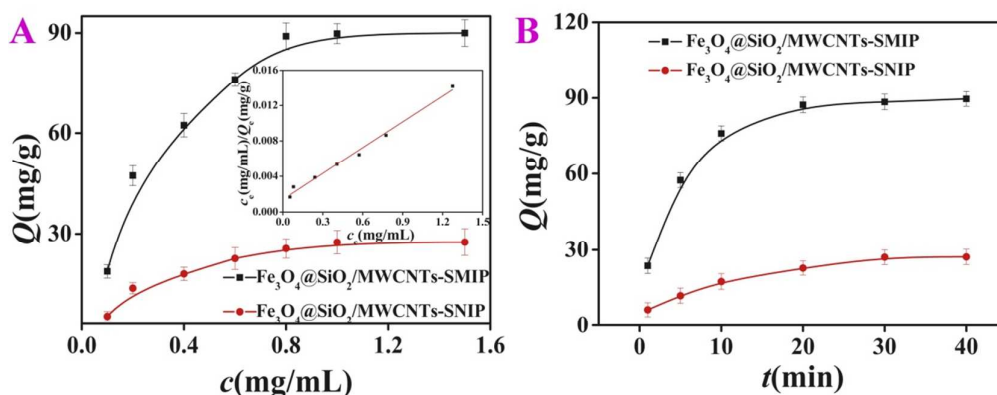
248

experimental result 91 mg/g.

249

The adsorption rate of Fe₃O₄@SiO₂/MWCNTs-SMIP and Fe₃O₄@SiO₂/

250 MWCNTs-SNIP to BHb, i.e. adsorption kinetics, was then studied and shown in Fig.
 251 5 (B). As we could observe in the figure, both the SMIP and SNIP particles could
 252 reach the maximum adsorption within 20 min for the imprinting cavities on the
 253 surface or in the proximity of the surface of $\text{Fe}_3\text{O}_4@\text{SiO}_2/\text{MWCNTs-SMIP}$ which
 254 could help mass transfer.



255

256

Fig.5. Adsorption isotherm curve of $\text{Fe}_3\text{O}_4@\text{SiO}_2/\text{MWCNTs-SMIP}$ and

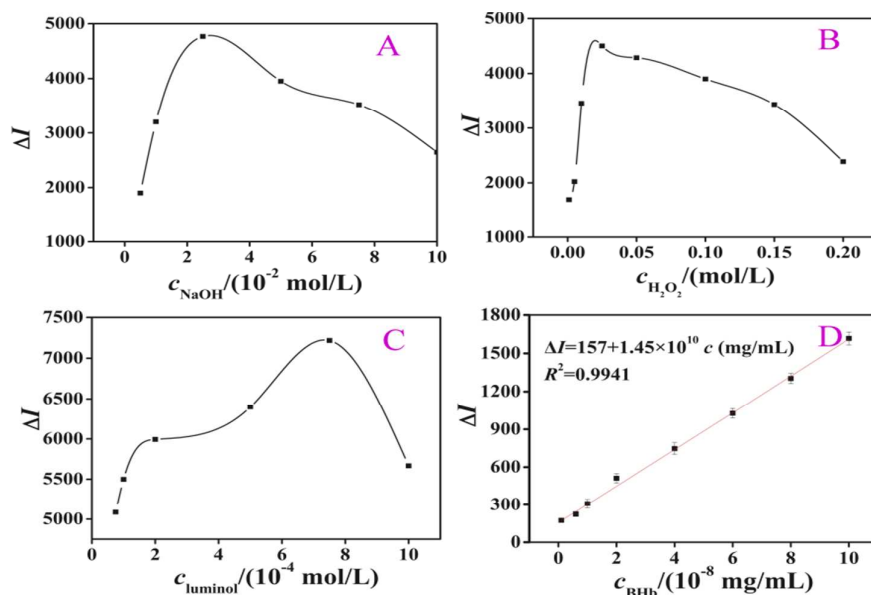
257 $\text{Fe}_3\text{O}_4@\text{SiO}_2/\text{MWCNTs-SNIP}$ (A). Adsorption kinetics curve of $\text{Fe}_3\text{O}_4@\text{SiO}_2/\text{MWCNTs-SMIP}$

258

and $\text{Fe}_3\text{O}_4@\text{SiO}_2/\text{MWCNTs-SNIP}$ (B)

259 3.3 Optimization of $\text{Fe}_3\text{O}_4@\text{SiO}_2/\text{MWCNTs-SMIP-CL}$ biosensor

260 Peristaltic pumps speed which determined the adsorption time to BHb was an
 261 important parameter in the experiment. While main pump speed and vice pump speed
 262 reached the best: 25 r/min, the effects of concentrations of hydrogen peroxide and
 263 sodium hydroxide on the CL reaction was researched. As shown in Fig. 6 (A-C), the
 264 optimal concentration conditions were 0.03 mol/L of NaOH solution, 0.04 mol/L of
 265 H_2O_2 solution and 7.2×10^{-4} mol/L of luminol solution, respectively.



266

267 **Fig.6.** Optimization results: (A) Effect of NaOH concentration on CL intensity. Conditions:268 $c(\text{H}_2\text{O}_2) = 0.1 \text{ mol/L}$, $c(\text{luminol}) = 1.0 \times 10^{-5} \text{ mol/L}$. (B) Effect of H_2O_2 concentration on CL269 intensity. Conditions: $c(\text{luminol}) = 1.0 \times 10^{-5} \text{ mol/L}$, $c(\text{NaOH}) = 0.03 \text{ mol/L}$. (C) Effect of luminol270 concentration on CL intensity. Conditions: $c(\text{H}_2\text{O}_2) = 0.04 \text{ mol/L}$, $c(\text{NaOH}) = 0.03 \text{ mol/L}$. (D) The271 regression equation of the $\text{Fe}_3\text{O}_4@\text{SiO}_2/\text{MWCNTs-SMIP-CL}$ biosensor272 **3.4 Analytical performance of the biosensor**273 The analytical performance of the described $\text{Fe}_3\text{O}_4@\text{SiO}_2/\text{MWCNTs-SMIP-CL}$ 274 biosensor was studied in the optical conditions ($c(\text{luminol}) = 7.2 \times 10^{-4} \text{ mol/L}$, $c(\text{H}_2\text{O}_2)$ 275 $= 0.04 \text{ mol/L}$, $c(\text{NaOH}) = 0.03 \text{ mol/L}$). The regression equation shown in Fig. 6 (D)276 was described by the calibration curve $\Delta I = 157 + 1.45 \times 10^{10} c$ (mg/mL , $R^2 = 0.9941$),277 and the detection range of BHB was from 5.0×10^{-10} to $7.0 \times 10^{-7} \text{ mg/mL}$. The278 detection limit was $1.7 \times 10^{-10} \text{ mg/mL}$ (3δ) with relative standard deviation (RSD) 4.9%279 ($n = 11$) by determination of $5.0 \times 10^{-8} \text{ mg/mL}$ BHB. The detection range and limit

280 was compared with traditional methods and the results were shown in Table 1. The

281 results showed that $\text{Fe}_3\text{O}_4@\text{SiO}_2/\text{MWCNTs-SMIP-CL}$ biosensor exhibited low

282 detection limit, high sensitivity and selectivity to BHB conceivably.

283

284 **Tab.1.** Comparing results with conventional methods

Method	Linear range (mg/mL)	Detection limit (mg/mL)
Our work	$5.0 \times 10^{-10} - 7.0 \times 10^{-7}$	1.7×10^{-10}
MIPs/AuE [5]	$1.0 \times 10^{-9} - 1.0 \times 10^{-3}$	
Fluorescence method [6]	$1.3 \times 10^{-3} - 0.13$	6.1×10^{-4}
Piezoelectric crystal immunosensor [7]	0.001-0.1	

285

286 **3.5 Interference study of the biosensor**

287 The detail information of interference study of the
 288 $\text{Fe}_3\text{O}_4@\text{SiO}_2/\text{MWCNTs-SMIP-CL}$ biosensor was shown in Table 2. The tolerable
 289 limit of coexisted species was less than $\pm 5\%$. In the CL biosensor, 150 times Na^+ and
 290 K^+ concentration (compared with BHB) interfered with the determination of BHB but
 291 when using $\text{Fe}_3\text{O}_4@\text{SiO}_2/\text{MWCNTs-SMIP}$ biosensor, 900 times Na^+ and K^+
 292 concentration would interfere with the determination of BHB for the imprinting
 293 cavities which were more adequate for macromolecule BHB and could recognize and
 294 absorb BHB specifically, while the interferences from BSA and Lys were serious
 295 relatively. It was shown that the BSA exhibited much more interference than Lys
 296 which was for that BSA had nearly the same size with BHB. Even so, from Table 2, it
 297 was easy to say that the application of $\text{Fe}_3\text{O}_4@\text{SiO}_2/\text{MWCNTs-SMIP}$ in CL biosensor
 298 could eliminate or reduce the interference.

299 **Tab.2.** The tolerable ratio of interfering species to BHB

Species	Na^+, K^+	Vanillin	Lys	BSA
$\text{Fe}_3\text{O}_4@\text{SiO}_2/\text{MWCNTs-SMIP-CL}$	900	700	100	40
CL	150	90	35	15

300

301 **3.6. Recyclability of $\text{Fe}_3\text{O}_4@\text{SiO}_2/\text{MWCNTs-SMIP}$ bioreceptor**302 The recyclability of $\text{Fe}_3\text{O}_4@\text{SiO}_2/\text{MWCNTs-SMIP}$ was an important parameter

303 of the biosensor, and it was evaluated by reusing $\text{Fe}_3\text{O}_4@\text{SiO}_2/\text{MWCNTs-SMIP}$. The
 304 BHB in used $\text{Fe}_3\text{O}_4@\text{SiO}_2/\text{MWCNTs-SMIP}$ was extracted with 0.5 mol/L NaCl and
 305 water respectively for 7 times for better binding capability to the BHB. It could be
 306 obtained that there was 7.1% binding capacity loss within 10 times of
 307 $\text{Fe}_3\text{O}_4@\text{SiO}_2/\text{MWCNTs-SMIP}$ to the concentration of 5.0×10^{-8} mg/mL BHB, which
 308 manifested that $\text{Fe}_3\text{O}_4@\text{SiO}_2/\text{MWCNTs-SMIP}$ was very suitable in the determination
 309 of BHB in practical samples directly.

310 3.7 Application of the biosensor

311 As shown in Table 3, $\text{Fe}_3\text{O}_4@\text{SiO}_2/\text{MWCNTs-SMIP-CL}$ biosensor was applied
 312 in biological samples which were made by mixing waste water containing unknown
 313 amount BHB in the optimal experimental conditions. Obviously, the recoveries from
 314 the samples were excellent and varied from 92% to 106%. These results showed that
 315 the biosensor had good accuracy to the determination of BHB. Therefore, the
 316 $\text{Fe}_3\text{O}_4@\text{SiO}_2/\text{MWCNTs-SMIP-CL}$ biosensor used for the determination of BHB was
 317 practical.

318 **Tab.3.** Application of biosensor

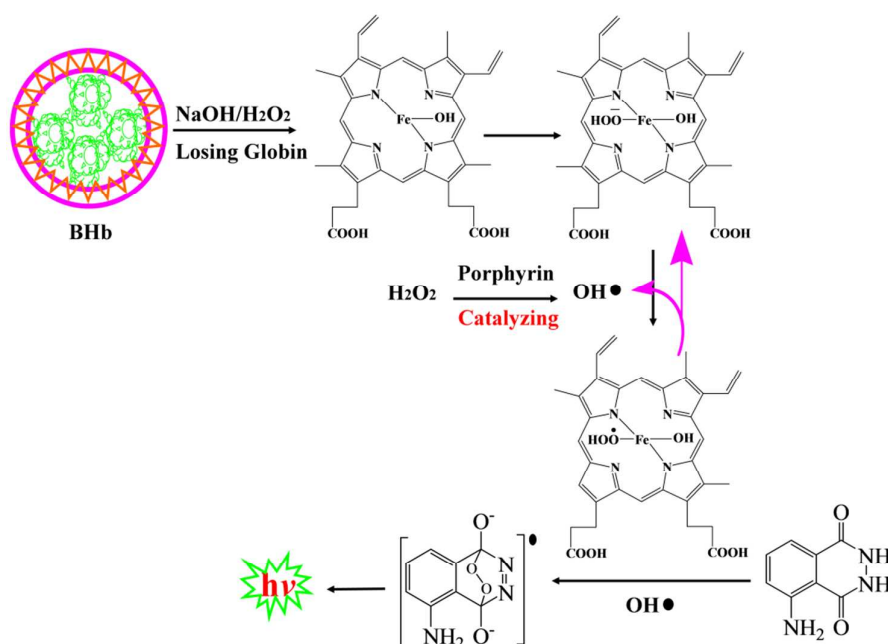
Sample	$c / (10^{-8} \text{ mg/mL})$ ($n=6$)	RSD%	Added(10^{-8} mg/mL)	Found(10^{-8} mg/mL) ($n=6$)	Recovery%
Sample 1 [#]	1.3	3.2	5.0	6.5	104
Sample 2 [#]	4.1	3.3	5.0	8.7	92
Sample 3 [#]	5.5	3.7	5.0	10.8	106
Sample 4 [#]	8.6	3.5	5.0	13.4	96

319

320 3.8 The possible CL mechanism of the biosensor

321 In alkaline condition, there was an overlapping broad absorption band of
 322 hemoglobin and hemin between 350 and 450 nm before oxidation in UV-vis spectra,

323 which would disappear when hemoglobin and hemin was oxidized. Hence, the
 324 possible CL mechanism of hemoglobin might be similar to that of hemin. In alkaline
 325 and H_2O_2 solution, by losing globin, hematin was generated. By analogy with the
 326 proposal for the porphyrin-catalyzed decomposition of peroxide into free radicals, a
 327 complexing of the peroxide with the central iron ion was formed in this reaction
 328 firstly [29]. Then, a heme-peroxy free radical was formatted. This radical could then
 329 act as the primary oxidant of luminol and increase its reactivity. Alternatively, the
 330 heme-peroxy free radical could dissociate to form a peroxy free radical which would
 331 function as the oxidant. Then, luminol was oxidized by $\text{HO}\cdot$ to be oxidized-state
 332 luminol which then returned to the ground-state and released photons. This could
 333 enhance the CL emission as shown in Fig.7.



334

335

Fig.7. The possible CL mechanism of the biosensor

336

4 Conclusion

337

338

339

In this work, based on $\text{Fe}_3\text{O}_4@\text{SiO}_2/\text{MWCNTs}$ as backbone materials to prepare SMIP bioreceptor, a CL biosensor for ultrasensitive determination of BHb was prepared. Compared with Arvand's et al. work [30], the prepared

340 $\text{Fe}_3\text{O}_4@\text{SiO}_2/\text{MWCNTs}$ with the new method was more stable on account of chemical
341 bond. Adsorption ability of the $\text{Fe}_3\text{O}_4@\text{SiO}_2/\text{MWCNTs}$ -SMIP was evaluated to be 91
342 mg/g. The $\text{Fe}_3\text{O}_4@\text{SiO}_2/\text{MWCNTs}$ -SMIP followed Langmuir isotherm equation and
343 exhibited excellent recognition and adsorption ability to BHB. Under the optimum
344 conditions of CL, the $\text{Fe}_3\text{O}_4@\text{SiO}_2/\text{MWCNTs}$ -SMIP-CL biosensor was very valuable
345 in determining BHB in samples with high selectivity and sensitivity.

346 **Acknowledgements**

347 This work was supported by the Shandong Provincial Natural Science Foundation of
348 China (No. ZR2012BM020) and the Scientific and technological development Plan
349 Item of Jinan City in China (No. 201202088).

350 **Reference**

- 351 1. Fan, X., et al., A green solid-phase method for preparation of carbon nitride
352 quantum dots and their applications in chemiluminescent dopamine sensing.
353 RSC Advances, 2015. **5**: p. 55158-55164.
- 354 2. Luaces, M.D., et al., Chemiluminescence analysis of enrofloxacin in surface
355 water using the tris(1,10-phenantroline)-ruthenium(II)/peroxydisulphate
356 system and extraction with molecularly imprinted polymers. Microchemical
357 Journal, 2013. **110**: p. 458-464.
- 358 3. G. Wulff, A.S., K. Zabrocki, Enzyme-analogue built polymers and their use
359 for the resolution of racemates. Tetrahedron Letters, 1973. **14**(44): p.
360 4329-4332.
- 361 4. Sellergren, B., Polymer- and template-related factors influencing the
362 efficiency in molecularly imprinted solid-phase extractions. Trac-Trends in
363 Analytical Chemistry, 1999. **18**(3): p. 164-174.
- 364 5. Keyes, M.H., D.E. Albert, and S. Saraswathi, Enzyme Semisynthesis by
365 Conformational Modification of Proteins. Annals of the New York Academy
366 of Sciences, 1987. **501**: p. 201-204.
- 367 6. Dabulis, K. and A.M. Klibanov, Molecular Imprinting of Proteins and Other
368 Macromolecules Resulting in New Adsorbents. Biotechnology and
369 Bioengineering, 1992. **39**(2): p. 176-185.
- 370 7. Shi, H.Q., et al., Template-imprinted nanostructured surfaces for protein
371 recognition. Nature, 1999. **398**(6728): p. 593-597.

- 372 8. Kato, M., et al., Polymerization of Methyl-Methacrylate with the
373 Carbon-Tetrachloride Dichlorotris(Triphenylphosphine)Ruthenium(Ii)
374 Methylaluminum Bis(2,6-Di-Tert-Butylphenoxide) Initiating System -
375 Possibility of Living Radical Polymerization. *Macromolecules*, 1995. **28**(5): p.
376 1721-1723.
- 377 9. Yildirim, E., E. Turan, and T. Caykara, Construction of myoglobin imprinted
378 polymer films by grafting from silicon surface. *Journal of Materials Chemistry*,
379 2012. **22**(2): p. 636-642.
- 380 10. Khezeli, T. and A. Daneshfar, Dispersive micro-solid-phase extraction of
381 dopamine, epinephrine and norepinephrine from biological samples based on
382 green deep eutectic solvents and Fe₃O₄@MIL-100 (Fe) core-shell
383 nanoparticles grafted with pyrocatechol. *RSC Advances*, 2015. **5**: p.
384 65264-65273.
- 385 11. Gao, R.X., et al., Preparation and characterization of uniformly sized
386 molecularly imprinted polymers functionalized with core-shell magnetic
387 nanoparticles for the recognition and enrichment of protein. *Journal of*
388 *Materials Chemistry*, 2011. **21**(44): p. 17863-17871.
- 389 12. He, H.Y., et al., Imprinting of protein over silica nanoparticles via surface
390 graft copolymerization using low monomer concentration. *Biosensors &*
391 *Bioelectronics*, 2010. **26**(2): p. 760-765.
- 392 13. Li, L., et al., Preparation of Core-shell Magnetic Molecularly Imprinted
393 Polymer Nanoparticles for Recognition of Bovine Hemoglobin. *Chemistry-an*

- 394 Asian Journal, 2009. **4**(2): p. 286-293.
- 395 14. Zhang, Z.H., et al., Novel magnetic bovine serum albumin imprinted polymers
396 with a matrix of carbon nanotubes, and their application to protein separation.
397 Analytical and Bioanalytical Chemistry, 2011. **401**(9): p. 2855-2863.
- 398 15. Scheller, F.W., et al., Thirty years of haemoglobin electrochemistry. Adv
399 Colloid Interface Sci, 2005. **116**(1-3): p. 111-20.
- 400 16. Fathallah, H., et al., Differences in response to fetal hemoglobin induction
401 therapy in beta-thalassemia and sickle cell disease. Blood Cells Mol Dis, 2009.
402 **43**(1): p. 58-62.
- 403 17. Wang, Y.Q., H.M. Zhang, and Q.H. Zhou, Studies on the interaction of
404 caffeine with bovine hemoglobin. Eur J Med Chem, 2009. **44**(5): p. 2100-5.
- 405 18. Luo, J., S.S. Jiang, and X.Y. Liu, Electrochemical sensor for bovine
406 hemoglobin based on a novel graphene molecular imprinted polymers
407 composite as recognition element. Sensors and Actuators B-Chemical, 2014.
408 **203**: p. 782-789.
- 409 19. Cai, D., et al., A molecular-imprint nanosensor for ultrasensitive detection of
410 proteins. Nature Nanotechnology, 2010. **5**(8): p. 597-601.
- 411 20. Li, D.Y., et al., Novel Hybrid Structure Silica/CdTe/Molecularly Imprinted
412 Polymer: Synthesis, Specific Recognition, and Quantitative Fluorescence
413 Detection of Bovine Hemoglobin. Acs Applied Materials & Interfaces, 2013.
414 **5**(23): p. 12609-12616.
- 415 21. Shao, B., et al., Determination of Bovine Hemoglobin by a Piezoelectric

- 416 Crystal Immunosensor. Fresenius Journal of Analytical Chemistry, 1993.
417 **346**(10-11): p. 1022-1024.
- 418 22. Zhao, Y.G., et al., Synthesis of amidoxime-functionalized Fe₃O₄@SiO₂
419 core-shell magnetic microspheres for highly efficient sorption of U(VI).
420 Chemical Engineering Journal, 2014. **235**: p. 275-283.
- 421 23. Lu, F.G., et al., Flow injection chemiluminescence sensor based on core-shell
422 magnetic molecularly imprinted nanoparticles for determination of
423 chrysoidine in food samples. Sensors and Actuators B-Chemical, 2012. **173**: p.
424 591-598.
- 425 24. Liang, D., et al., Selective oxidation of glycerol with oxygen in a base-free
426 aqueous solution over MWNTs supported Pt catalysts. Applied Catalysis
427 B-Environmental, 2011. **106**(3-4): p. 423-432.
- 428 25. Ai, L.H. and J. Jiang, Removal of methylene blue from aqueous solution with
429 self-assembled cylindrical graphene-carbon nanotube hybrid. Chemical
430 Engineering Journal, 2012. **192**: p. 156-163.
- 431 26. Liu, H.F., et al., Synthesis of TiO₂/SiO₂@Fe₃O₄ magnetic microspheres and
432 their properties of photocatalytic degradation dyestuff. Catalysis Today, 2011.
433 **175**(1): p. 293-298.
- 434 27. Zhang, M., et al., The preparation of magnetic molecularly imprinted
435 nanoparticles for the recognition of bovine hemoglobin. Talanta, 2014. **120**: p.
436 376-385.
- 437 28. Jia, X.P., et al., Polydopamine-based molecular imprinting on silica-modified

- 438 magnetic nanoparticles for recognition and separation of bovine hemoglobin.
439 Analyst, 2013. **138**(2): p. 651-658.
- 440 29. T. P. Vasileff, G.S., H. A. Neuffld, L. Spero, Hemin as a Catalyst for
441 Chemiluminescence. *Experientia*, 1974. **30**(1): p. 20-22.
- 442 30. Arvand, M. and M. Hassannezhad, Magnetic core-shell
443 Fe₃O₄@SiO₂/MWCNT nanocomposite modified carbon paste electrode for
444 amplified electrochemical sensing of uric acid. *Materials Science &*
445 *Engineering C-Materials for Biological Applications*, 2014. **36**: p. 160-167.